JOURNAL OF GEOPHYSICAL RESEARCH, VOL. 104, NO. D16, PAGES 19,071–19,083, AUGUST 27, 1999

A statistical modeling approach for the simulation of local paleoclimatic proxy records using general circulation model output

Bernhard K. Reichert and Lennart Bengtsson
Max-Planck-Institut für Meteorologie, Hamburg, Germany

Ove Åkesson
Swedish Meteorological and Hydrological Institute, Norrköping

Abstract. A statistical modeling approach is proposed for the simulation of local paleoclimatic proxy records using general circulation model (GCM) output. A method for model-consistent statistical downscaling to local weather conditions is developed which can be used as input for process-based proxy models in order to investigate to what extent climate variability obtained from proxy data can be represented by a GCM, and whether, for example, the response of glaciers to climatic change can be reproduced. Downscaling is based on a multiple linear forward regression model using daily sets of operational weather station data and large-scale predictors at various pressure levels obtained from reanalyses of the European Centre for Medium-Range Weather Forecasts. Composition and relative impact of predictors vary significantly for individual stations within the area of investigation. Owing to a strong dependence on individual synoptic-scale patterns, daily data give the highest performance which can be further increased by developing seasonal-specific relationships. The model is applied to a long integration of a GCM coupled to a mixed layer ocean (ECHAM4/MLO) simulating present-day and preindustrial climate variability. Patterns of variability are realistically simulated compared to observed station data within an area of Norway for the period 1868-1993.

1. Introduction

Understanding spatiotemporal patterns and mechanisms of natural climate variability, as well as the anthropogenic impact on climate, requires the extension of instrumental records further back in time by the usage of paleoclimatic proxy data. Several attempts to reconstruct reliable temperature patterns over the last few centuries have been made [e.g., *Landsberg et al.*, 1978; *Groveman and Landsberg*, 1979; *Bradley and Jones*, 1993; *Barnett et al.*, 1996; *Bradley*, 1996; *Mann et al.*, 1998]. Proxy records obtained from ice cores [e.g., *Thompson*, 1982], tree rings [e.g., *Briffa et al.*, 1992] and corals [e.g., *Dunbar et al.*, 1994], as well as historical data [e.g., *Pfister*, 1992] and long instrumental records [e.g., *Jones and Bradley*, 1992] have been used to reconstruct large-scale or global-scale patterns. Valley glaciers [e.g., *Oerlemans*, 1992, 1997] can also provide important information on the evolution of the regional or local climate.

How can these proxy data best be interpreted and what are the underlying forcing mechanisms? Recent interpretation studies [*Mann et al.*, 1998] have investigated the influence of external forcings, such as solar irradiance variations and explosive volcanism on Northern Hemispheric temperature variations. General circulation models (GCMs) [e.g., *Roeckner et al.*, 1996; *Manabe and Stouffer*, 1996] integrated over a long period of time could contribute as they are an important tool for analyzing mechanisms underlying the climate system behavior and the role of forcing factors. However, a different methodology for a systematic evaluation of paleoclimatic proxy data is then required as will be proposed in this paper.

The question we would like to address is whether we are able to simulate "synthetic" paleoclimatic proxy records from GCM output for comparison with actual in situ proxy data. Our strategy is to perform a model-consistent statistical downscaling of the output of a GCM combined with a process-based forward modeling approach to simulate, for example, the behavior of valley glaciers and the growth of trees under specific conditions. Simulated records can be compared to actual in situ proxy records in order to investigate whether, for example, the response of glaciers to climatic change can be reproduced by models, and to what extent climate variability obtained from proxy records (with the main focus on the last millennium) can be interpreted.

The growth of a valley glacier is mainly controlled by local temperature and precipitation [*Paterson*, 1981; *Oerlemans*, 1996]. Such data are very difficult to obtain from grid-point-scale GCM output because of very large deviations due to local orographic conditions. As will be shown in this paper, a careful statistical model derived from the present climate can provide reliable local data which can be used to force the

Paper number 1999JD900264.
0148-0227/99/1999JD900264$09.00

growth of such a valley glacier. A similar downscaling approach is required, and can be developed, for the evaluation of dendrochronological data.

One of the initial studies addressing the method of statistical downscaling is the work of *Kim et al.* [1984]. Monthly surface temperature and precipitation for stations in Oregon are analyzed for the purpose of relating their distributions to large-scale monthly anomalies. Downscaling is addressed here as "the statistical problem of climate inversion". Later, the approach is modified [*Wigley et al.*, 1990] and applied to predict meteorological variables for a number of selected sites in the United States [*Karl et al.*, 1990]. The method is used to predict regional precipitation changes over the Iberian peninsula [*von Storch et al.*, 1993] and to downscale monthly mean North Atlantic air pressure to sea level anomalies in the Baltic Sea [*Heyen et al.*, 1996] using monthly mean predictor data. A comparison of three methods of downscaling [*Cubasch et al.*, 1996] shows that direct interpolation of GCM grid points gives a poor representation of the local climate and that statistical downscaling is an appropriate and inexpensive tool for regions with sufficient observational data to train the model. In a study by *Martin et al.* [1996], GCM output is downscaled to simulate the snow climatology of the French Alps based on an analog procedure which associates a real meteorological situation to model output.

The method of statistical downscaling that is used in this study uses daily operational weather station data and a large set of potential large-scale predictors obtained from daily European Centre for Medium-Range Weather Forecasts (ECMWF) reanalyses [*Gibson et al.*, 1997] in order to develop robust statistical relationships between the large-scale flow and local variables. Specific questions investigated in this study concern the role of near-surface predictors (section 5.1) and the spatial homogeneity of the statistical model (section 5.3), as well as its performance on single seasons which are most important for a specific proxy indicator (section 5.4). Can we, for example, obtain from a GCM reliable local summer temperatures for the growing season of trees, and which predictors do we need in order to do so? Further questions concern the importance of horizontal GCM resolution and the time sampling for the determination of suitable predictors (section 5.6). It is found, for example, that daily data sets for the development of the statistical model give the closest and most robust relations due to a strong dependence on individual synoptic-scale patterns.

2. General Strategy

The general strategy proposed in this paper is the following (Figure 1). First we develop a statistical model between daily large-scale circulation patterns and corresponding local data observed by operational weather stations located near a proxy site to be investigated. Large-scale patterns are represented by daily ECMWF reanalyses (ERA) for the period 1979-1993. We use daily data in order to include synoptic timescale variability and to achieve physically robust relations (see section 5.6). The obtained statistical relationships are applied to the daily coarse spatial grid point output of a GCM in order to achieve local GCM output (statistical downscaling). A forward modeling approach for a specific proxy, for example, a glacier model [*Oerlemans*, 1996], can then be used to produce "synthetic" (paleoclimatic) proxy data which finally can be compared to actual in situ proxy data.

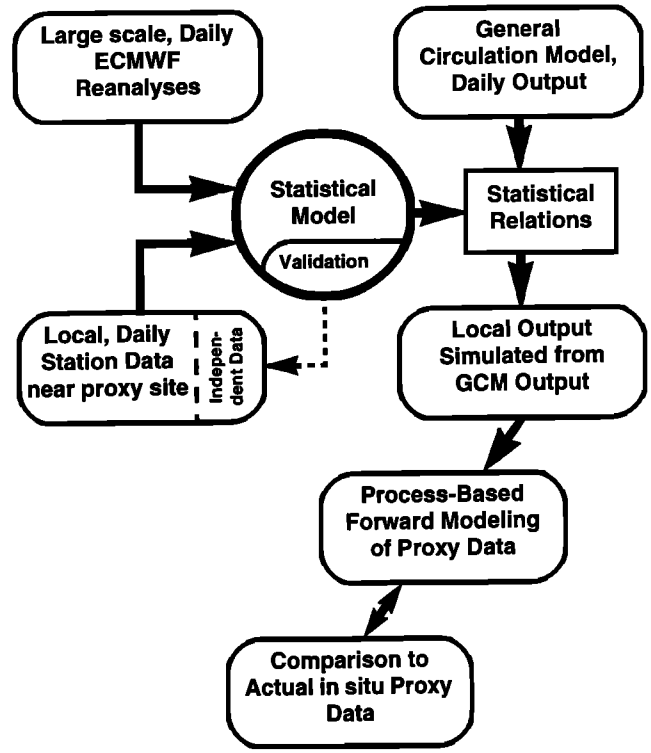

Figure 1. General strategy for the interpretation and usage of in situ paleoclimatic proxy data as proposed in this paper. See text for further explanations.

3. Statistical Model

The response of local weather to large-scale flow patterns of the atmosphere has been noted for a very long time, not only by meteorologists, but also by laymen interested in weather. The most common feature is perhaps the precipitation in mountainous regions which is particularly determined by orographic forcing, generating enhanced precipitation on the windward and reduced precipitation on the leeward side. In most areas the local conditions (topography and land surface characteristics) have a major effect not only on precipitation but also on wind and temperature as well as on cloudiness and visibility. *Bergeron* [1930] (see also *Bengtsson* [1981]) proposed that a special climatology should be established classifying local climate in terms of the large-scale flow. This approach may be identified as a dynamic climate classification. The significance of this approach became obvious as it became possible to predict the synoptic flow by numerical models. A dynamic climatology can be produced for any particular local weather parameter (predictand), for example, local precipitation, cloud cover, cloud height, visibility, and maximum or minimum temperature, by the use of different large-scale predictors, for example, surface pressure, wind, geopotential thickness, vertical velocity, and large-scale precipitation.

For the purpose of this analysis we use a multiple linear forward regression model in order to establish relations between the large-scale flow and local weather parameters.

For the $i = 1, 2, ..., n$ values of an observed (dependent) quantity y_i (predictand) it takes the form of a linear combination

$$y_i = \beta_0 x_{i0} + \beta_1 x_{i1} + \beta_2 x_{i2} + ... + \beta_p x_{ip} + \varepsilon_i \quad (1)$$

where $x_{i0} = 1$ and $x_{i1}, x_{i2}, ..., x_{ip}$ are the settings of the p corresponding (independent) quantities (predictors), $\beta_0, \beta_1, ..., \beta_p$ are the regression parameters which are to be estimated, and ε_i are unknown independent random errors (see, for example, *von Storch and Zwiers* [1999]). We use least squares estimation, which means that best estimates of the unknown regression parameters are calculated by minimizing

$$\Sigma_{i=1}^{n} \varepsilon_i^2 \quad (2)$$

for each predictand.

However, it is neither necessary nor desirable to include all potential predictors in the data set for the prediction of a specific observed local variable. The maximum number of predictors that may be used in the model in order to get a "stable" solution which not only fits the developmental sample but also works on independent data sets is a function of the sample size. Furthermore, some predictors included in the model might be a linear or "near-linear" combination of other predictors (collinearity or "near-collinearity"). which could cause unstable results. In order to address these problems, we choose the following selection procedure for the large daily data set that is used in this study: The model is built up stepwise using an interactive forward selection procedure of independent variables. After having chosen a single predictor with maximum correlation, the next independent variable providing the best fit in conjunction with the first one is added and tested for near-collinearity. In a critical case the user may decide whether this variable should be included or not. Further variables are added in a recursive fashion until a saturation criterion (the correlation does not improve significantly) is reached.

4. Data Sets: ECMWF Reanalyses and Observed Data

The development of the statistical model is based on ECMWF reanalyses (ERA) [*Gibson et al.*, 1997] used for an area of about 11° x 11° in Norway (covering the proxy site of Nigardsbreen glacier at 61°43'N, 7°08'E to be investigated) and on local observational records for 22 synoptic weather stations within that area.

4.1. ECMWF Reanalyses (Predictors)

The ECMWF reanalysis project has produced a validated and reasonably consistent global data set of assimilated data for the period 1979-1993 [*Gibson et al.*, 1997]. In this study, ERA data constitute the potential predictors for the development of the statistical model. We use ERA 24 hour forecasts for precipitation in order to address the spin-up problem and to have a consistent picture of precipitation [*Stendel and Arpe*, 1997]. For all other surface and pressure level variables (Table 1), 6 hourly initialized analyses are taken and daily averaged. We extract pressure level variables on the 1000, 925, 850, 700, 500, 400, and 300 hPa levels.

Composite predictors (Table 1) are calculated directly from ERA data. "Geopotential $a - b$ hPa" means geopotential height on level a minus geopotential height on level b (geopotential thickness). The four "seasonal cycle" functions are potential predictors to account for seasonal-specific features while establishing the statistical model between large-scale predictors and local observations. "Seasonal cycle: cos(day)" represents a cosine function with a period of 1 year. It is calculated for each day of the year and has a maximum (+1) at January 1 and a minimum (-1) at July 1. It is the most relevant "seasonal cycle" predictor for the statistical model. For the prediction of local temperature, it might be used in order to enhance or weaken the seasonal cycle that appears, for example, in the ERA large-scale 850 hPa temperature. "Seasonal cycle: sin(day)" is a sine function with a period of 1 year and a maximum at April 1 and a minimum at October 1. "Seasonal cycle: sin(2·day)" is a sine function with a period of half a year and maxima at February 15 and August 15 and minima at May 15 and November 15. "Seasonal cycle: cos(2·day)" is a cosine function with a period of half a year and maxima at January 1 and July 1 and minima at April 1 and October 1. Further composite predictors are the sum of large-scale and convective precipitation in the ERA output (total precipitation), the square root of total precipitation, the vertically integrated liquid water content (total column water minus total column water vapor), the temperature lapse rate of the lower troposphere (linear regression between temperatures on the geopotential heights of the 1000, 925, 850, and 700 hPa levels) and the K index as an atmospheric stability index [*George*, 1960].

Before applying ERA output to the statistical model, it is interpolated to T30 (~ 3.8° x 3.8°) resolution in order to meet the resolution of the European Center/Hamburg (ECHAM)

Table 1. Large-Scale Predictors From ECMWF Reanalyses

Predictor Type	Predictors
Pressure level predictors (1000, 925, 850*, 700*, 500*, 400*, 300* hPa)	temperature*, dew point temperature*, u wind velocity*, v wind velocity*, vertical velocity*, vorticity*, divergence*, geopotential height*, relative humidity*
Surface predictors	large-scale precipitation, convective precipitation, mean sea level pressure*, total cloud cover, total column water vapor
Composite predictors†	geopotential thickness at 925-1000, 850-1000, 700-1000, 500-1000, 500-850*, 500-700* hPa, seasonal cycle: sin(day)*, seasonal cycle: cos(day)*, seasonal cycle: sin(2·day)*, seasonal cycle: cos(2·day)*, large-scale+convective precipitation, square root of total precipitation, vertically integrated liquid water, lapse rate of the lower troposphere (see text), K index [*George*, 1960]

*The model version excluding near-surface predictors (see text) uses exclusively potential predictors on the 850, 700, 500, 400, and 300 hPa levels, mean sea level pressure, geopotential thickness, and the "seasonal cycle" predictors (predictors marked with asterisks).

†See text for definition of composite predictors.

GCM runs which we intend to use afterward. For each location of the operational weather stations we compute weighted area means for an area covering roughly 1200 km x 1200 km (corresponding to nine grid points in T30 resolution) as input for the statistical model. Additional experiments with original T106 (~ 1.1° x 1.1°) resolution of ERA output (using 16 grid points to cover the area of investigation) are also analyzed (see section 5.6).

4.2. Observed Station Data (Predictands)

The predictands (dependent variables) of the model consist of observational data for 22 operational weather stations (see Figure 2 for locations) in the vicinity of Nigardsbreen glacier, Norway. Most stations (exceptions: 02 Hustad-Nerland, 03 Reimegrend, 08 Tynkrysset, 22 Eidfjord-Bu, 23 Sognefjell Mountain) cover the period 1979-1993. We interpolate missing values in the 6 hourly weather data before daily averaging. However, data quality is adequate for most stations in that period and only a few data are missing. Table 2 shows the observed parameters used as input for the statistical model. Composite predictands (Table 2) are logarithm, square root as well as cube and fourth root of observed 24 hour precipitation (prediction of local precipitation may be improved using these predictands), u wind and v wind components (calculated from wind direction and wind velocity), and relative humidity (calculated from temperature and dew point temperature).

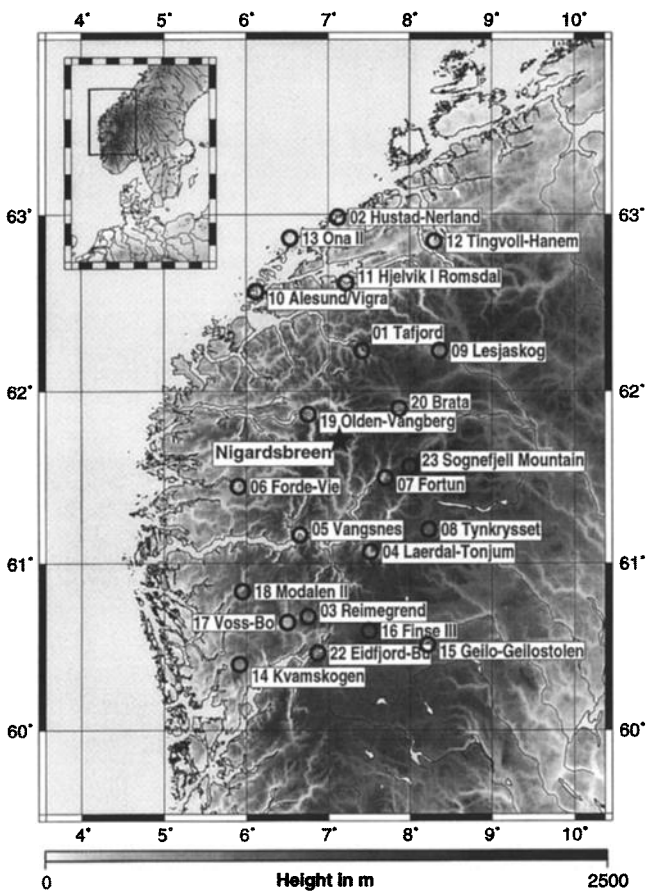

Figure 2. Location of operational weather stations used for development of the statistical model. We anticipate being able to provide reliable local outputs for the Nigardsbreen valley glacier (61°43'N, 7°08'E).

Table 2. Predictands From Observed Weather Station Data

Predictand Type	Predictands
Observed predictands	pressure reduced, wind direction, wind velocity, temperature, dew point temperature, 24 hour precipitation, total cloud amount
Composite predictands†	logarithm, square root, cube, and fourth root of 24 hour precipitation, u wind component, v wind component, relative humidity

Results only for a selection of these parameters will be presented in this paper.

†See text for definition of composite predictands.

5. Results of Statistical Modeling

The complete data set that can potentially enter the statistical model consists of daily values of 76 large-scale potential predictors from ECMWF reanalyses and 14 observed local predictands for the period 1979-1993, which means about 5500 daily sets of 90 variables for each of the 22 stations.

5.1. Role of Near-Surface Predictors

In order to investigate the role of near-surface predictors for the statistical model, we choose two different model versions. In the first one, we allow all predictors (complete Table 1) to potentially enter the equations. The predictors which are finally selected by the model represent only a small subset of these variables; for local precipitation, for example, usually not more than five large-scale predictors play a significant role and are therefore actually used. In the second one we only use potential predictors above the 850 hPa level (850, 700, 500, 400, and 300 hPa), mean sea level pressure, and the seasonal cycle (noted by asterisks in Table 1). Here, near-surface predictors are excluded in order to be able to get stable results even when applying the model to various GCMs which might differ in the underlying topography and in the representation of surface processes. It is found that the correlation between observed and predicted variables in this model only slightly decreases compared to the first model version, which suggests that predictors above the 850 hPa level are already sufficient for the prediction of the desired local surface variables. The large-scale variability of the synoptic timescale flow is well determined from predictors above the 850 hPa level.

5.2. General Model Performance

Figures 3a - 3f show an example of statistical model output for the Norwegian station Kvamskogen (60°24'N, 5°55'E, 408 m above sea level). Here, we perform the statistical model on a daily basis with reanalyses at T30 resolution including predictors above 850 hPa only (second model version) for the period 1979-1992. The shaded curves show large-scale direct reanalyses for the station without statistical

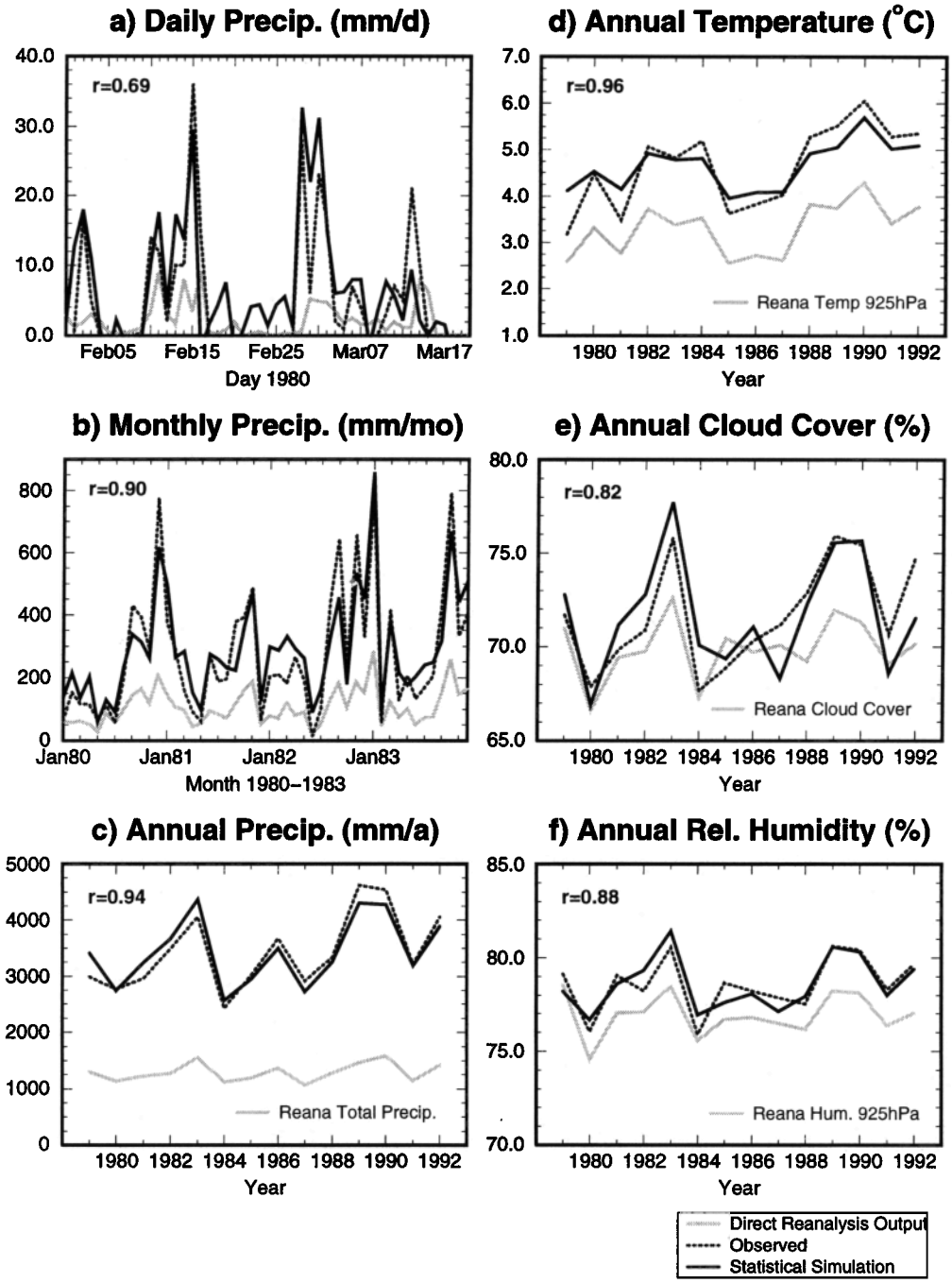

Figure 3. Results of the statistical model for station Kvamskogen (60°24'N, 5°55'E, 408 m above sea level, station 14 in Figure 2). Local output is shown for (a) daily precipitation, February 1 to March 19, 1980, (b) monthly precipitation, January 1980 to December 1983, (c-f) annual precipitation, temperature, total cloud cover, and relative humidity, 1979-1992. Solid lines show statistically simulated results, dotted lines represent observed data, and shaded lines are directly interpolated reanalyses without statistical modeling. The correlation coefficient r is shown in the top left corner of each graph (see text).

modeling, the solid curves represent statistically simulated results, and the dotted curves show observational data. The correlation coefficient r is shown in the top left corner of each graph.

The station is generally characterized by an exceptionally high amount of observed precipitation (up to 4000 mm/yr) which can naturally not be represented by the direct large-scale reanalysis precipitation (about 1300 mm/yr).

In order to achieve the best fit, the statistical model finally selects three large-scale predictors for the prediction of local precipitation (Table 3). These can be found in the upper right part of Table 3 together with their relative impacts in the final

Table 3. Predictors Selected by the Statistical Model and Percentage of Observed Variance Explained

Local Temperature: Predictors and Relative Impact for Complete Years 1979-1992	Local Precipitation: Predictors and Relative Impact for Complete Years 1979-1992
temperature at 850 hPa relative impact 65%	vertical velocity at 850 hPa relative impact 60%
seasonal cycle: cos(day) relative impact 25%	vorticity at 700 hPa relative impact 20%
relative humidity at 850 hPa relative impact 10%	zonal wind at 700 hPa relative impact 20%

	Total Explained Variance for Local Temperature			Total Explained Variance for Local Precipitation		
	Daily	Monthly	Annual	Daily	Monthly	Annual
Year	(91.3%)	85.0%	91.9%	47.7%	81.7%	88.6%
JJA	69.8%	79.4%	77.5%	29.6%	57.2%	46.0%
DJF	71.7%	93.5%	95.7%	59.9%	90.1%	94.0%

The predictors are shown with their individual relative impact in the final equations for local temperature and local precipitation for station Kvamskogen using daily data for complete years within the period 1979-1992 (see section 4.1 for further explanation of the "seasonal cycle" predictor). The bottom part of the table shows the percentage of observed variance explained by the statistical model for the whole year, June, July, and August (JJA) only, and December, January, and February (DJF) only each for original daily data, monthly-averaged output of the statistical model after removing the seasonal cycle, and yearly means of statistical model output (which means seasonally averaged output in the case of JJA and DJF).

equations. The predictors enter the equations such that (1) negative vertical velocity (upward air movement at 850 hPa, relative impact 60%), (2) positive u-wind velocity (westerly winds at 700 hPa, relative impact 20%) and (3) positive vorticity (cyclonic movement at 700 hPa, relative impact 20%) on the large scale determine an increase of local precipitation, which for this station is strongly orographically enhanced. Using these three predictors exclusively, the explained variance (r^2) between the statistical simulation and the observed record of precipitation is 47.7% for daily data for the complete years 1979-1992 (bottom right part of Table 3).

This value can be further analyzed by investigating the skill of the model for each season individually. The explained variance for daily data in summer (June, July, August (JJA); Table 3, bottom right) is rather low (29.6%) compared to the winter (December, January, February (DJF)) value (59.9%). Also monthly means (57.2% compared to 90.1% in winter) and seasonal means (46.0% compared to 94.0% in winter) remain low. The reason for that might be that the amount of precipitation in summer is smaller (see Figure 4a) and less strongly coupled to atmospheric dynamics than in winter. In summer we believe that convective precipitation has a much higher impact, which weakens the skill of the statistical model using large-scale predictors as input. Figure 3a shows an example of daily precipitation in February/March 1980 for periods where the model does not produce enough precipitation (e.g., around March 13) and periods where actually nonexistent precipitation is generated (e.g., within the period February 17 to February 27 no precipitation was observed). However, the explained variance for monthly means for the complete year is as high as 81.7% (Figure 3b for 1980-1983); annual means (Figure 3c) even show a remarkable explained variance of 88.6%. This means that monthly and annual mean precipitation is realistically simulated by the statistical model (Figure 3c) on the basis of daily input values.

Further experiments with monthly and yearly values show that daily values are required to obtain such robust and physically reasonable couplings. Local climatic conditions can be modeled well using daily large-scale predictors. However, the orographic effect plays an important role and is perhaps the easiest to determine, especially in wintertime with pronounced synoptic flow.

Figures 3d, 3e, and 3f show the model results for annual means of temperature, cloud cover, and relative humidity, respectively. The predictors chosen for local temperature (Table 3, upper left) are large-scale temperature at 850 hPa with the highest relative impact (65%), followed by the seasonal cycle (25%; see section 4.1 concerning "seasonal cycle: cos(day)") and relative humidity at 850 hPa (10%). The explained variance of 91.3% for daily data (Table 3, bottom left) is not representative because it includes the seasonal cycle. However, monthly data can explain 85% of the variance after removing the seasonal cycle, and yearly data can explain as much as 91.9%. The explained variance of annual total cloud cover (67.2%; Figure 3e) is also improved compared to the direct large-scale reanalyses. The same is true for annual relative humidity (Figure 3f) compared to reanalyses relative humidity on 925 hPa.

Figure 4 shows the climatologies for the period 1979-1992 of precipitation (Figure 4a) and temperature (Figure 4b) each for observed station data, statistical simulations, and directly interpolated reanalysis output. Although we do not have a perfect match between observed data and simulated output for precipitation (Figure 4a), it is clearly visible how the seasonal cycle is enhanced and the climatology is improved compared to direct reanalysis output. This is also true for temperature (Figure 4b). The seasonal cycle of large-scale temperature is modified and matches the observed one nearly perfectly, also demonstrating the qualitative influence of the "seasonal cycle" predictor (see section 4.1).

This is just one example out of all stations used in this study. The following section provides information on the skill of the model for other stations within the area of investigation.

5.3. Spatial Homogeneity of the Statistical Model

The statistical model may use different optimized predictors with varying relative impacts for the same observed variable at each station due to its local setting. This is demonstrated for 17 stations in the area of Nigardsbreen glacier, Norway. Figure 5 shows the explained variances for observed local temperature (Figure 5a) and observed local precipitation (Figure 5b) for each operational weather station (see Figure 2 for locations; five stations did not cover the ERA time period and are not used, see section 4.2). They

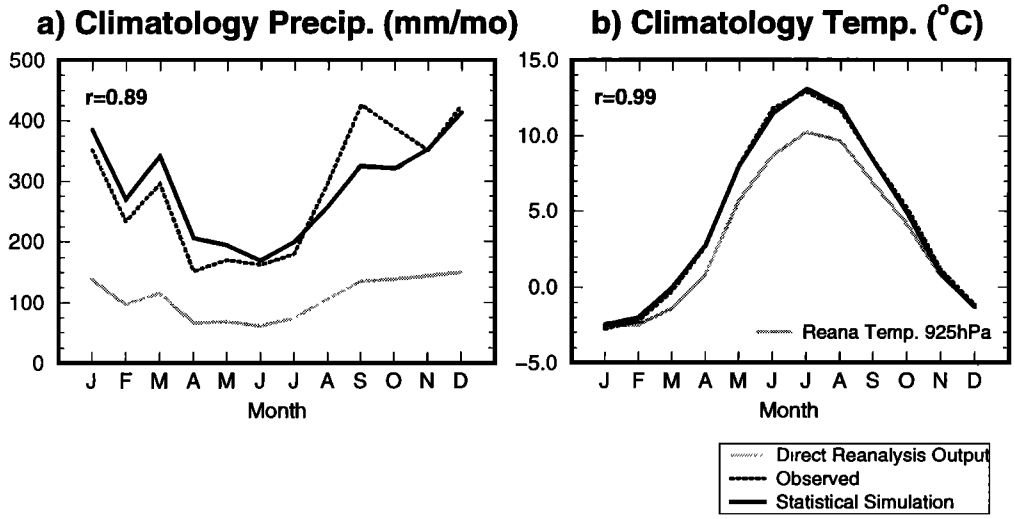

Figure 4. Climatology for the period 1979-1992 of (a) precipitation and (b) temperature for observed station data (dotted lines), statistically simulated output (solid lines) and direct reanalysis output (shaded lines) for station Kvamskogen. The correlation coefficient r is shown in the top left corner of each graph.

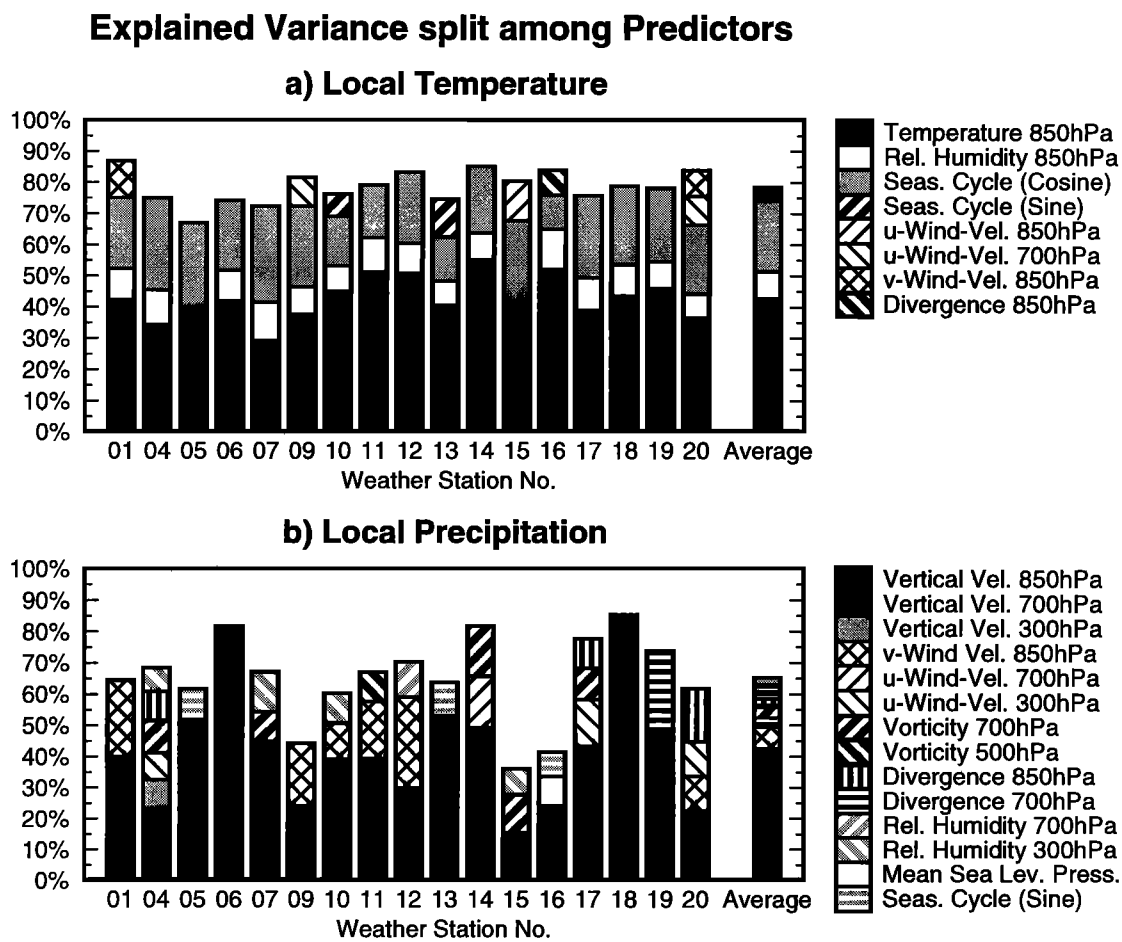

Figure 5. Explained variances of the statistical model for (a) observed local temperature and (b) observed local precipitation for each weather station (see Figure 2 for location of stations). The explained variances are split among the large-scale predictors from ECMWF reanalyses chosen by the model.

were calculated using monthly-averaged values after removing the seasonal cycle, and they are split among the large-scale predictors from ECMWF reanalyses chosen by the statistical model. Also shown is the average of explained variance over all stations and its composition.

In general, spatial homogeneity for temperature (Figure 5a) is much higher than for precipitation, as can be expected. The dominant predictors for local temperature are large-scale temperature at 850 hPa, the seasonal cycle (see section 4.1 concerning "seasonal cycle: cos(day)"), and relative humidity at 850 hPa with an averaged explained variance of 42.7%, 22.6%, and 8.7%, respectively. Although large-scale temperature has a dominant influence in the equations, its monthly climatology is modified by the "seasonal cycle" predictor as has already been mentioned in section 5.2 (Figure 4b). Without including this predictor, the simulation changes qualitatively, and the explained variance decreases significantly. With the daily large-scale temperature predictor alone we would not achieve the maximum skill of the statistical model. On average, 78.6% of observed local temperature could be explained by the statistical model for all stations.

The explained variance and composition of predictors for local precipitation (Figure 5b) varies significantly for each station. The predictors selected by the statistical model and their impact can be completely different even for stations that are located close to each other (see, e.g., stations 04 and 05). This is due to their local setting, which is crucial for precipitation. With respect to total explained variance, we may divide the stations into three groups. Stations 18, 14, 06, 17, and 19 belong to the first group with the highest total explained variance (more than 80% on average). These stations are mainly located in the west of the area to be investigated (see Figure 2). The most dominant predictor is by far vertical velocity at 850 hPa, explaining 61.6% of observed variance on average. Remarkably, for stations 18 and 06 it is also the only predictor selected by the statistical model. This demonstrates the strong coupling of local precipitation to atmospheric dynamics. Further predictors with smaller influence on particular stations are divergence, vorticity, and wind velocity at varying pressure levels. The second group consists of stations 12, 04, 11, 07, 01, 13, 05, 20, and 10 with total explained variances that are close to the average of 65.2% over all stations. These stations are mainly located in the middle and in the north of the area. Besides vertical velocity at 850 hPa, v wind velocity at 850 hPa also plays an important rule for some of these stations. For stations 12 and 01, as much as 30% and 24% of variance, respectively, can be explained by this predictor; westerly winds are associated with an increase of precipitation here. For the third group of stations, the total explained variances of only 44%, 41%, and 36% (stations 09, 16, and 15, respectively) are far below the average over all stations. There is no obvious reason for that; either data quality of measurements has an influence here, or it is just impossible to find better large-scale predictors for these local settings out of the set of 76 variables from ECMWF reanalyses using the linear regression model.

Besides giving insights into spatial homogeneity of the statistical model, this section demonstrates the need for the statistical modeling procedure itself. This also becomes clear by the following experiments: We run the statistical model using additional potential surface predictors including large-scale and convective precipitation from ECMWF reanalyses (model version 1, see section 5.1). Then, the precipitation predictors are either not even selected by the model for the simulation of local precipitation (true for most stations), or the impact of these predictors is extremely small. That means that just by using the direct grid point output of reanalyses (this is, of course, also true for the output of GCM experiments), it is impossible to have a realistic picture of local precipitation. For the simulation of local temperatures, the situation is less extreme, but they are also improved qualitatively compared to the direct grid point output of a model (especially the seasonal cycle; see section 5.2). This is due to the inclusion of additional predictors and the adaptation to the local setting of a station including the orography. For the simulation of a valley glacier, for example, both local temperature (including seasonality) and precipitation are crucial, and the statistical modeling procedure as proposed here is therefore essential.

It should be mentioned that we do not claim that this approach will work equally well in any other part of the world. However, we have carried out further experiments for an area surrounding an Austrian valley glacier in the Alps (Hintereisferner; 46.80°N, 10.93°E) with comparably good results, and we have planned further experiments for other locations.

5.4. Model Runs for Specific Seasons of the Year

Is it possible that different predictors may be required for different seasons of the year? The simulation of proxy indicators may require realistic local output with a particular interest in specific seasons (e.g., the growing season of trees or the melting period of glaciers). In order to further investigate the seasonal performance of the statistical model, we carried out experiments allowing daily data for single seasons only as input (Table 4). Compared to the model with full year daily input (Table 3), the composition of predictors and their individual impacts may change.

1. With regard to JJA temperatures, if we restrict input data to daily values of JJA (Table 4) then local JJA temperatures are determined by large-scale zonal wind at 850 hPa (relative impact 17%) and vertical velocity at 500 hPa (relative impact 12%), in addition to 850 hPa temperature (relative impact 71%). Here, the daily, monthly, and seasonal explained variance for JJA is 81%, 91.8%, and 89.1%, respectively (bottom part of Table 4). Compared to the seasonal performance with full year input (69.8%, 79.4%, and 77.5%; Table 3, bottom part) the explained variances improve significantly and the predictors have changed.

2. With regard to DJF temperatures, the explained variance for Northern Hemispheric winter (75.8% in Table 4 with daily DJF input data only) is slightly improved compared to the full year input (71.7% in Table 3), whereas monthly and seasonal values remain nearly constant. This means that the large-scale flow patterns in wintertime are already reasonably well determined by the full year input data.

For the prediction of local precipitation, experiments with daily data for specific seasons are also carried out. Although the complete set of potential large-scale predictors (Table 1, predictors marked with asterisks) is offered to the statistical model (as usual), the composition of selected predictors for summer (JJA) precipitation remains the same as for the full year input (Table 3). Also, the total explained variance of 29.7% for daily data remains almost constant (compared to 29.6% in Table 3), demonstrating that even the season-

Table 4. Predictors Selected and Performance of the Season-Specific Statistical Model for Local Temperature

Local Temperature: Predictors and Relative Impact for JJA Only 1979-1992			Local Temperature: Predictors and Relative Impact for DJF Only 1979-1992		
temperature at 850 hPa relative impact 71%			temperature at 850 hPa relative impact 60%		
zonal wind at 850hPa relative impact 17%			relative humidity at 850 hPa relative impact 24%		
vertical velocity at 500 hPa relative impact 12%			zonal wind at 500 hPa relative impact 16%		
Total Explained Variance for Local Temperature, JJA Only			Total Explained Variance for Local Temperature, DJF Only		
Daily	Monthly	Annual	Daily	Monthly	Annual
81.0%	91.8%	89.1%	75.8%	94.5%	95.6%

The model was developed with daily reanalyses and weather station data using JJA values only and DJF values only within the period 1979-1992 (see text and Table 3 for further explanations). The bottom part of the table shows the percentage of observed variance explained by the statistical model for JJA only and DJF only each for original daily data, monthly averaged output of the statistical model after removing the seasonal cycle, and seasonal means of statistical model output.

specific statistical model is not able to improve the relations between large-scale variables and local summer precipitation. As mentioned in section 5.2, we believe that this is due to the relatively large contribution of convective precipitation in summer, which weakens the skill of the statistical model using large-scale predictors as input. For winter (DJF) precipitation the statistical model again selects vertical velocity at 850 hPa with a relative impact of 66% (compared to 60% for the full year input, Table 3). In contrast to the full year model run, it also selects vorticity at 850 hPa (relative impact 19%) and temperature at 400 hPa (relative impact 15%). However, in spite of the fact that the predictors are modified to maximize the skill of the model in winter, the total explained variance is not significantly improved; it remains at 60.8% for daily data (compared to 59.9%, Table 3). That means that for our experiments with our set of potential predictors, the quality of simulations for local precipitation is not seasonally dependent as for local temperature. Predictors selected for the full year already seem to be optimized even for the simulation of individual seasons.

We may conclude that for selected observed variables (valid for local temperature but not for local precipitation), the capability to simulate individual seasons can be improved significantly by developing a season-specific statistical model.

5.5. Model Validation Experiments

Does the model work on independent data, and is it transferable to other time periods with different climatic conditions? In order to address these questions, two further experiments are carried out.

In the first experiment we develop the model for the second half of the ECMWF reanalyses time period (1985-1992) only (Figure 6). For the purpose of validation, the statistical relationships obtained are then applied to an independent validation sample, in this case the first half of the reanalyses time period (1979-1984). The annual means of precipitation and temperature for this experiment are shown in Figures 6a and 6b. For temperature (Figure 6b), statistical simulations and observed data are of the same order of magnitude for the developmental and validation sample (also comparable to Figure 3d using the full time period 1979-1992 for development). For precipitation (Figure 6a) the model shows a slightly enhanced output in the validation sample. The tendency to produce too much precipitation in this period can already be seen in the experiment using the full time period 1979-1992 for development (Figure 3c) but is enhanced here. However, the model is able to simulate the local variables for this independent validation sample rather realistically, although it is not developed for this time period (i.e., it does not use any local observations in the period 1979-1984 for fitting).

The second experiment addresses the question of whether the model can produce realistic output for events which differ from events the model is actually developed for. These events would occur in slightly changed climatic conditions (which are not fundamentally different in their large-scale flow properties, see below and section 6). If the model is developed using present-day climatic conditions (represented by ECMWF reanalyses), is it then applicable to GCM output for preindustrial times? The statistical distribution of daily local temperatures for station Kvamskogen after statistical modeling of ECMWF reanalyses for the period 1979-1992 is shown in Figure 7. The standard experiment (Figure 7a) includes all temperature events occurring for the development of the model. For the validation experiment (Figure 7b), events with temperatures less than -5°C are excluded prior to model development; afterward the statistical relationships are calculated the same way. Although this model is not developed for these events it has still realistically simulated them, which can be clearly seen in the distribution (Figure 7b, top graph) and the time series (Figure 7b, bottom graph) of temperatures. The differences between the standard and validation experiment (Figure 7a and 7b respectively) are reasonably small. This shows that, as long as the extreme events do not correspond to fundamentally different (and possibly nonlinear) weather regimes, then the statistical model is still able to simulate them. This is to a large extent true for the events of the preindustrial output of the GCM (see section 6) which will be applied below. Here, the general coupling between the large-scale flow and local weather parameters deduced from present-day climate is to a great extent maintained.

The two described experiments demonstrate the applicability of the statistical model to independent data sets, and they also show that we may simulate events which have not been visited in the developmental time period as far as the events do not correspond to fundamentally different (and possibly nonlinear) weather regimes.

5.6. Impact of Spatiotemporal Resolution of Predictors

Our intention is to produce reliable local monthly or annual mean output from reanalyses and GCMs comparable to

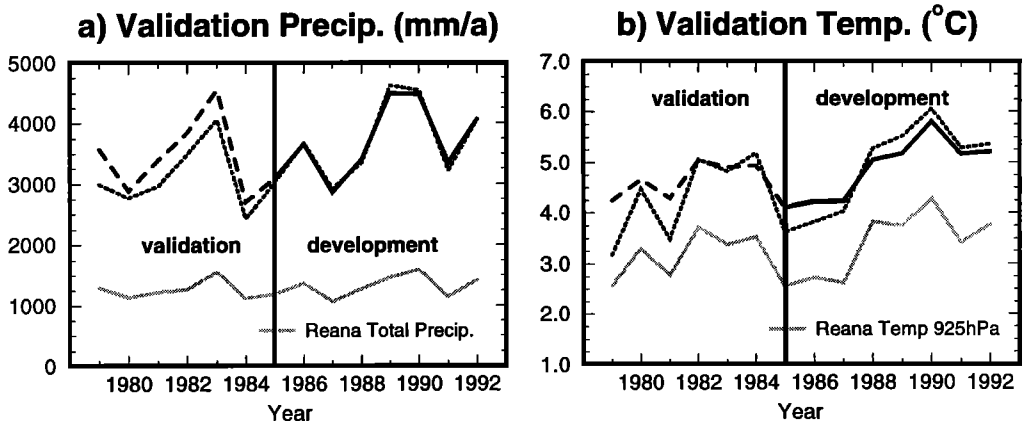

Figure 6. Validation experiment for station Kvamskogen (a) for local annual precipitation and (b) for local annual temperature. The model is developed for the 1985-1992 period only (developmental sample). The statistical relationships obtained are then applied to independent reanalyses for 1979-1984 (validation sample). The solid and dashed lines show the statistical model output for the developmental and validation sample, respectively, dotted lines represent observed data, and shaded lines are directly interpolated reanalyses without statistical modeling. See Figures 3c and 3d (using full time period 1979-1992 for development) for comparison.

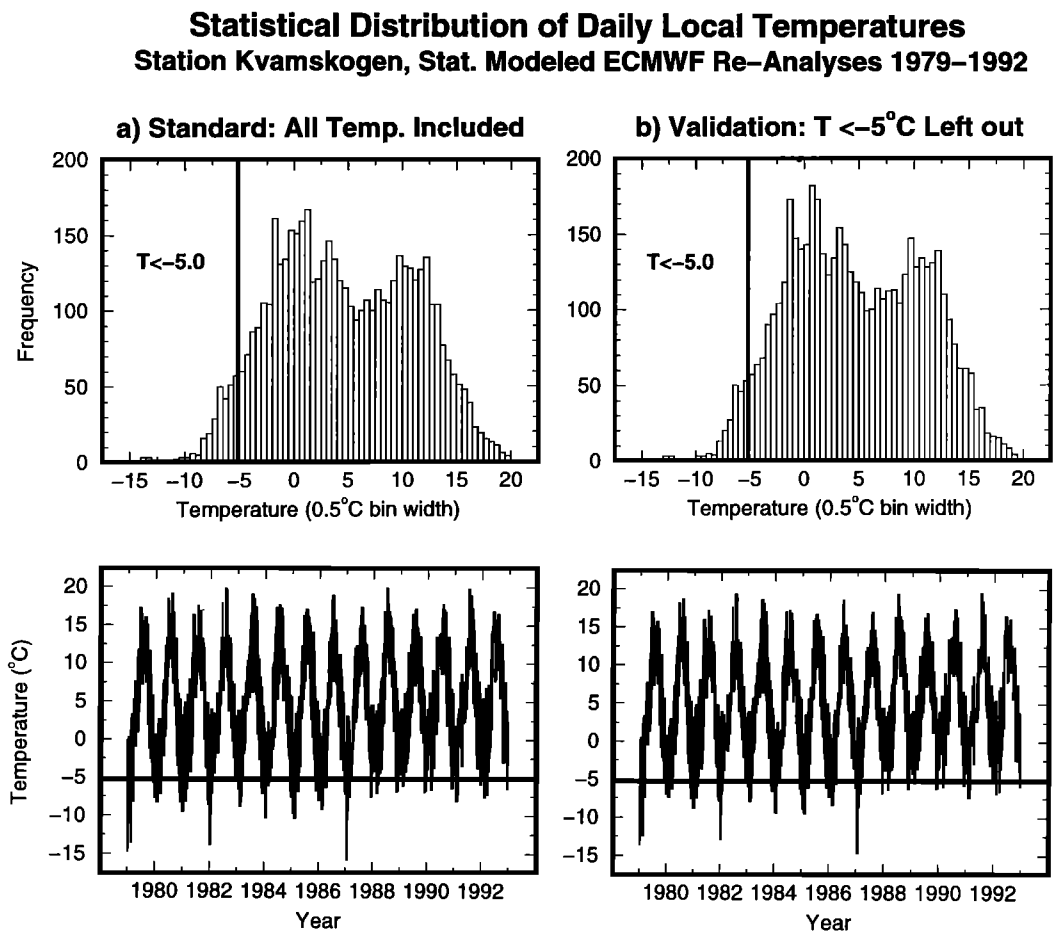

Figure 7. Statistical distribution (top graph) of daily local temperatures for station Kvamskogen after statistical modeling for the period 1979-1992 and time series of daily temperatures (bottom graph) for (a) all temperature events included for the development of the model and (b) events with temperatures less than -5°C excluded from model development. Although the model in Figure 7b is not developed for events < -5°C it still has realistically simulated them; the differences in distribution between Figures 7a and 7b are reasonably small. This shows that, as long as the extreme events do not correspond to a fundamentally different weather regime, then the statistical model is still able to simulate them.

corresponding local weather station data. Although we do not aim to produce perfect predictions on a daily basis, it turns out that our model requires daily predictor data as input in order to achieve the statistically closest and most robust relationships. Consequently, the output can best be averaged to monthly or annual means after the statistical calculations have been carried out using daily predictor data.

Monthly means as input are tested as well, but the results are less good. The model sometimes attempts to use near-collinear predictors for least squares estimation, which particularly becomes a problem when being applied to independent data. Furthermore, the actual physical relations between large-scale flow and local variables cannot be represented as satisfactorily as for daily data as input; a lot of information is averaged out. This is especially important for the simulation of local precipitation; the model has no choice other than to select predictors which represent much less meaningful physical relations to the large-scale flow compared to daily data as input.

This emphasizes the role of synoptic timescale variability in the close relations between local weather and large-scale circulation patterns. Averaging the predictors means that this information is partly removed and the correlation therefore weakens.

The impact of spatial resolution of predictors is investigated, producing statistical model output both using large-scale predictors (see section 4.1 for definition) from the interpolated T30 data set (~ 3.8° x 3.8°) and using original reanalyses at T106 resolution (~ 1.1° x 1.1°) for comparison. Although the interpolated reanalyses would maybe not be completely similar to the output of an imaginable reanalyses project using T30 resolution from the beginning, they are suitable to give us information on the impact of model resolution. It is found that summer temperatures (JJA) are most sensitive. For the example given in Table 3, the explained variance of monthly data for JJA (seasonal cycle removed) is increased from 79.4% (T30 resolution) to 84.5% (T106 resolution); annual data improve from 77.5% (T30 resolution) to 83.3% (T106 resolution). The sensitivity for local precipitation is of the same order. Monthly means for JJA increase from 57.2% (Table 3) to 62.1%, annual means from 46.0% to 51.7%. The improvements are not more drastic since even at T106 resolution, the predictors still represent the large-scale flow which is already well represented at T30 resolution for the area to be investigated.

In spite of these improvements, we may conclude that the overall ability to produce satisfactory statistical model output is already given using T30 predictor resolution, which is also the resolution of the ECHAM4 GCM runs which will be used below.

6. Application to ECHAM4 GCM: Control and Preindustrial Run

The statistical relationships derived from ECMWF reanalyses and local station data are applied to the output of the ECHAM4 general circulation model coupled to a mixed layer ocean (ECHAM4/MLO) developed at the Max-Planck-Institut für Meteorologie (MPI) and the Deutsches Klimarechenzentrum (DKRZ) in Hamburg [*Roeckner et al.*, 1996; *Roeckner*, 1997; *Roeckner et al.*, 1999]. We use a long integration of a control run and a run with constant preindustrial greenhouse gas concentrations for our experiments. The control experiment of the 19-layer ECHAM4/MLO GCM has been performed for 590 years at T30 (~ 3.8° x 3.8°) resolution. The concentrations of carbon dioxide, methane, and nitrous oxide are fixed at the observed 1990 values [*Intergovernmental Panel on Climate Change (IPCC)*, 1990, Table 2.5]. A 100-year equilibrium run with constant preindustrial greenhouse gas concentrations [*IPCC*, 1995] has also been performed. The global average surface air temperature for the preindustrial run in equilibrium is 1.0°C lower than for the control run.

The daily large-scale output of these models for the area of Nigardsbreen glacier, Norway, is applied to the statistical relationships obtained as described above. As an example, we show the statistically downscaled and yearly-averaged GCM output of surface air temperature deviations for station Ona II (Figure 8). This station is chosen because we are able to compare the variability of simulated data to a long instrumental observed temperature record for the period 1868-1955 which is available from the Global Historical Climatology Network (GHCN) temperature data base [*Peterson and Vose*, 1997]. Additionally, we include weather station data for the period 1979-1993 obtained from the Swedish Meteorological and Hydrological Institute (SMHI) for this station. We have subtracted the mean value of the latter data both from GHCN and SMHI data. The middle plot of Figure 8 shows the observed temperature deviations at station Ona II. The left and right plots of Figure 8 represent statistically corrected GCM surface air temperature output with constant preindustrial greenhouse gas concentrations and statistically corrected GCM output for 590 years of the control run, respectively.

In general, we assume that the statistical relationships (established by the linear regression model for present-day climate on a daily basis) between large-scale circulation patterns and local parameters are maintained when applying the statistical model to preindustrial times. A comparison of circulation patterns of the preindustrial GCM run with the control run supports this assumption. However, this might not be valid for climates with major changes in the general circulation (e.g., simulation for Last Glacial Maximum), for which the composition and impact of large-scale predictors might differ significantly.

The first striking feature is the mean temperature difference of about 0.8°C between the preindustrial GCM run and the control run, which is comparable to the observed temperature increase over the last 125 years for this station. This is due to the realistic large-scale GCM output itself within this region, but it also shows that the statistical model (besides improving the variability of local records) is capable of maintaining mean large-scale temperature changes due to different climatic conditions for this location.

More important for the performance of the statistical model is that the annual variability in GCM output (both control and preindustrial run) closely resembles the observed one. The standard deviation for the 100-year preindustrial run and the 590-year control run is 0.49 and 0.53, respectively, compared to 0.57 for the observed temperature record. The dynamical GCM output in combination with the statistical modeling procedure therefore seems to be a realistic simulation. However, when comparing a GCM simulation in equilibrium state (constant greenhouse gas concentrations) with observations, it is, of course, possible that the variability is affected by the fact that greenhouse gases are continuously increasing. Experiments with transient coupled GCM runs

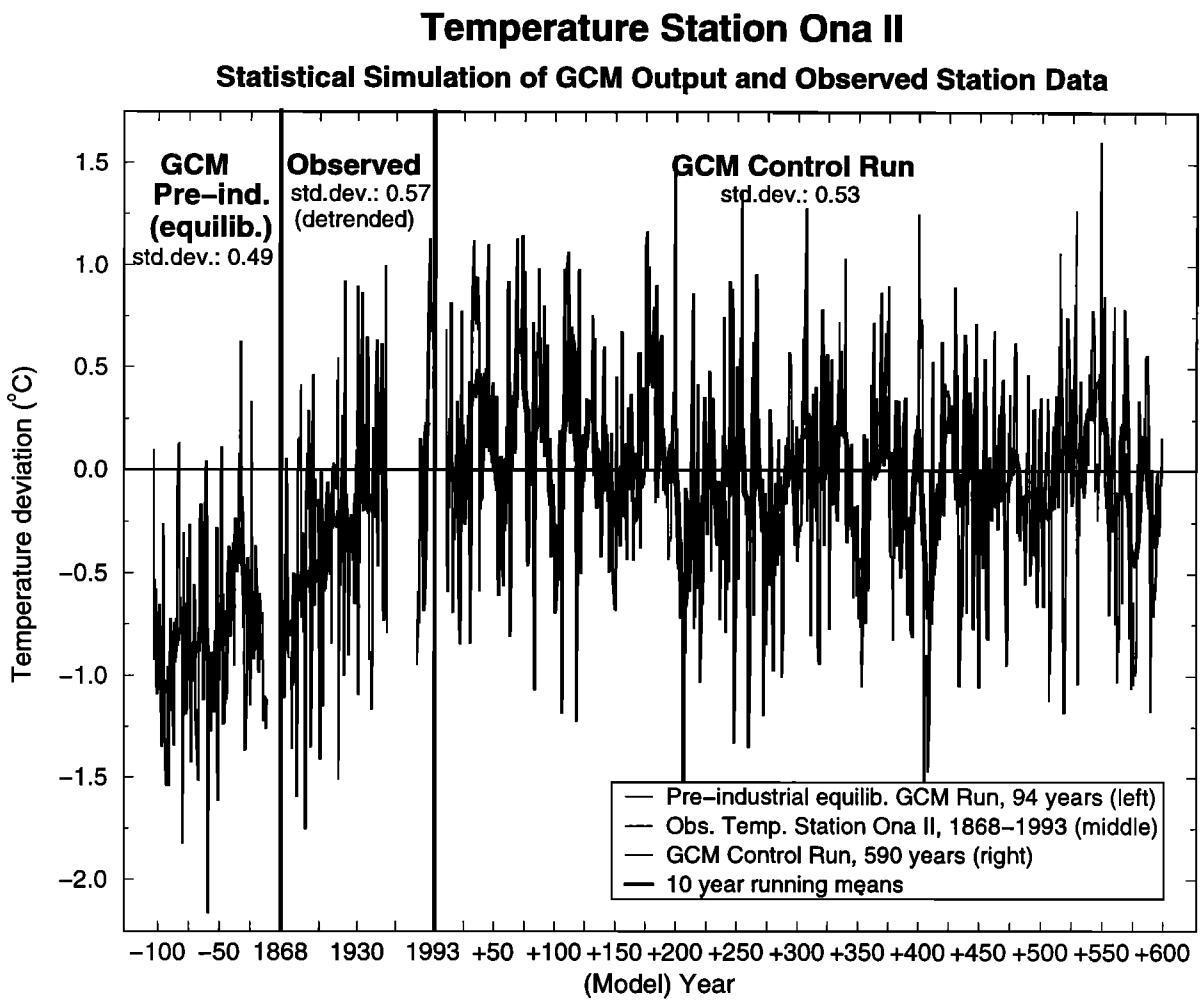

Figure 8. Application of the statistical model to GCM output (ECHAM4 T30 L19 Mixed Layer Ocean) for station Ona II. Thin lines are annual mean temperature deviations; thick lines are 10-year running means. The left plot shows statistically corrected local output from the equilibrium GCM run with constant preindustrial [*IPCC*, 1995] greenhouse gas concentrations; the right plot represents the 590-year control run of the same model with modern greenhouse gas concentrations. For comparison, observed temperature deviations for Station Ona II are shown in the middle plot.

(ECHAM4/OPYC3) will therefore also be performed in future.

The 10-year running means of the GCM simulations show a comparable or even slightly higher variability than in the relatively short observational record of 125 years. Pronounced lower-frequency fluctuations are clearly simulated by the downscaled GCM control experiment.

We may conclude that the statistically modeled dynamical GCM output can realistically simulate both the patterns of observed variability on the annual to decadal scale as well as temperature changes due to different climatic scenarios.

7. Conclusions

Local output for temperature, precipitation, and other parameters has been produced by a general circulation model in combination with a statistical downscaling model. Stable and physically reasonable relationships for statistical model development were obtained using large-scale predictors from daily ECMWF reanalyses and local surface observations for the area of Nigardsbreen glacier, Norway. Near-surface predictors were excluded in order to be able to get stable results even when applying the model to various GCMs which might differ in the underlying topography and in the representation of surface processes. Investigating the spatial homogeneity of the model showed that the composition of predictors and their relative impact varies significantly for individual stations within the area to be investigated due to their local setting. Analyzing single seasons individually, it became clear that for some local surface variables it is useful to develop a specific set of predictors for seasons which might be most relevant for a specific proxy indicator (e.g., for the growing season of trees). Daily predictor data were required in order to achieve statistically the most stable and physically the most reasonable relationships. Satisfactory results for the model could be achieved using T30 resolution (~ 3.8° x 3.8°) predictor data. We validated the model using separate developmental and validation intervals for the reanalyses time period and we carried out a validation experiment with a restricted predictor data set. The method has been applied to a long control integration of the ECHAM4 / Mixed Layer Ocean GCM and to an equilibrium run with preindustrial greenhouse gas forcing. The output has been compared to patterns of observed station data in the area of Nigardsbreen glacier, Norway, for the period 1868-1993. Patterns of observed variability on the annual to decadal scale

and temperature changes due to the preindustrial climatic scenario have been realistically simulated for this location.

The proposed dynamical-statistical modeling approach could help to improve a systematic interpretation of paleoclimatic proxy records and model-data intercomparisons for past climatic scenarios. A simulation of the growth of trees and the response of valley glaciers to specific climatic conditions is in preparation.

Acknowledgments. The authors would like to thank M. Giorgetta, M. Stendel, E. Roeckner and B. Machenhauer for helpful comments and discussions. The ECMWF provided the reanalyzed data set, the SMHI contributed operational weather station data, and NOAA made GHCN data available. The study was supported by the European Commission under contract ENV4-CT95-0072. The model simulations were performed at the Deutsches Klimarechenzentrum (DKRZ) in Hamburg.

References

Barnett, T.P., B. D. Santer, P. D. Jones, R. S. Bradley, and K. R. Briffa, Estimates of low frequency natural variability in near-surface air temperature, *Holocene, 6*, 255-263, 1996.

Bengtsson, L., The weather forecast, *Pure Appl. Geophys., 119*, 515-537, 1981.

Bergeron, T., Richtlinien einer dynamischen Klimatologie, *Meteorol. Z., 47*, 246-262, 1930. (Engl. transl., Ground plan of a dynamic climatology, *Mon. Weather Rev., 59*, 219-235, 1931.)

Bradley, R. S., Are there optimum sites for global paleotemperature reconstruction?, in *Climatic Variations and Forcing Mechanisms of the Last 2000 Years*, edited by P. D. Jones, R. S. Bradley and J. Jouzel, *NATO ASI Ser., Ser. I, 41*, 603-624, 1996.

Bradley, R. S., and P. D. Jones, "Little Ice Age" summer temperature variations: Their nature and relevance to recent global warming trends, *Holocene, 3*, 367-376, 1993.

Briffa, K. R., P. D. Jones, T. S. Bartholin, D. Eckstein, F. H. Schweingruber, W. Karlen, P. Zetterberg, and M. Eronen, Fennoscandian summers from AD 500: Temperature changes on short and long timescales, *Clim. Dyn., 7*, 111-119, 1992.

Cubasch, U., H. von Storch, J. Waszkewitz, and E. Zorita, Estimates of climate change in southern Europe derived from dynamical climate model output, *Clim. Res., 7*, 129-149, 1996.

Dunbar, R. B., G. M. Wellington, M. W. Colgan, and P. W. Glynn, Eastern Pacific sea surface temperature since 1600 A.D., The $d^{18}O$ record of climate variability in the Galapagos corals, *Paleoceanography, 9*, 291-315, 1994.

George, J. J. (Ed.), *Weather Forecasting for Aeronautics*, pp. 407-415, Academic, San Diego, Calif., 1960.

Gibson, J. K., P. Kållberg, S. Uppala, A. Nomura, A. Hernandez, and E. Serrano, ERA Description, *ECMWF Re-Anal. Proj. Rep. Ser., Rep. 1*, Eur. Cent. for Medium-Range Weather Forecasts, Reading, England, 1997.

Groveman, B. S., and H. E. Landsberg, Reconstruction of Northern Hemisphere temperature: 1579-1880, in *Meteorol. Program Publ., vol. 79-181*, Univ. of Md., College Park, 1979.

Heyen, H., E. Zorita, and H. von Storch, Statistical downscaling of monthly mean North Atlantic air-pressure to sea level anomalies in the Baltic Sea, *Tellus, Ser. A, 48*, 312-323, 1996.

Intergovernmental Panel on Climate Change (IPCC), *Climate Change, The IPCC Scientific Assessment*, edited by J. T. Houghton et al., Cambridge Univ. Press, New York, 1990.

IPCC, *Climate Change 1994, Radiative Forcing of Climate Change*, edited by J. T. Houghton et al., p. 80/194, Cambridge Univ. Press, New York, 1995.

Jones, P. D., and R. S. Bradley, Climatic variations in the longest instrumental records, in *Climate Since A. D. 1500*, edited by R. S. Bradley and P. D. Jones, pp. 246-268, Routledge, New York, 1992.

Karl, T. R., W.-C. Wang, M. E. Schlesinger, R. W. Knight, and D. Portman, A method of relating general circulation model simulated climate to the observed local climate, I, Seasonal statistics, *J. Clim., 3*, 1053-1079, 1990.

Kim, J.-W., J.-T. Chang, N. L. Baker, D. S. Wilks, and W. L. Gates, The statistical problem of climate inversion: Determination of the relationship between local and large-scale climate, *Mon. Weather Rev., 112*, 2069-2077, 1984.

Landsberg, H. E., B. S. Groveman, and I. M. Hakkarinen, A simple method for approximating the annual temperature of the Northern Hemisphere, *Geophys. Res. Lett., 5*, 505-506, 1978.

Manabe, S., and R. J. Stouffer, Low-frequency variability of surface air temperature in a 1000-year integration of a coupled atmosphere-ocean-land surface model, *J. Clim., 9*, 376-393, 1996.

Mann, M. E., R. S. Bradley, and M. K. Hughes, Global-scale temperature patterns and climate forcing over the past six centuries, *Nature, 392*, 779-787, 1998.

Martin E., B. Timbal, and E. Brun, Downscaling of general circulation model outputs - Simulation of the snow climatology of the French Alps and sensitivity to climate change, *Clim. Dyn., 13*, 45-56, 1996.

Oerlemans, J., Climate sensitivity of glaciers in southern Norway: Application of an energy-balance model to Nigardsbreen, Helstugubreen and Alfotbreen, *J. Glaciol., 38*, 223-232, 1992.

Oerlemans, J., Modelling the response of valley glaciers to climatic change, in *Physics and Chemistry of the Atmospheres of the Earth and Other Objects of the Solar System*, edited by C. Boutron, Eur. Res. Course Atmos., vol.2, pp. 91-123, Les Editions de Physique, Les Ulis, France, 1996.

Oerlemans, J., A flow-line model for Nigardsbreen: Projection of future glacier length based on dynamic calibration with the historic record, *Ann. Glaciol., 24*, 382-389, 1997.

Paterson, W. S. B. (Ed.), *The Physics of Glaciers*, 2nd ed., Pergamon, New York, 1981.

Peterson, T. C., and R. S. Vose, An overview of the Global Historical Climatology Network temperature data base, *Bull. Am. Meteorol. Soc., 78*, 2837-2849, 1997.

Pfister, C., Monthly temperature and precipitation in central Europe from 1525-1979: Quantifying documentary evidence on weather and its effects, in *Climate Since A. D. 1500*, edited by R. S. Bradley and P. D. Jones, pp. 118-142, Routledge, New York, 1992.

Reichert, B. K., L. Bengtsson, and O. Åkesson, A statistical-dynamical modeling approach for the simulation of local paleo proxy records using GCM output, *Rep. 274*, Max-Planck-Inst. für Meteorol., Hamburg, Germany, 1998.

Roeckner, E., L. Arpe, L. Bengtsson, M. Christoph, M. Claussen, L. Dumenil, M. Esch, M. Giorgetta, U. Schlese, and U. Schulzweida, The atmospheric general circulation model ECHAM-4: Model description and simulation of present-day climate, *Rep. 218*, Max-Planck-Inst. für Meteorol., Hamburg, Germany, 1996.

Roeckner, E., Climate sensitivity experiments with the MPI/ECHAM4 model coupled to a slab ocean (abstract), in *Euroclivar Workshop on Cloud Feedbacks and Climate Change*, edited by C. A. Senior and J. F. B. Mitchell, pp. 20, Hadley Cent. for Clim. Predict. and Res., Bracknell, England, 1997.

Roeckner, E., Bengtsson, L., Feichter, J. Lelieveld, J. and H. Rodhe, Transient climate change simulations with a coupled atmosphere-ocean GCM including the tropospheric sulfur cycle, *J. Clim.*, in press, 1999.

Stendel, M., and K. Arpe, Evaluation of the Hydrological Cycle in Re-Analysis and Observations, ECMWF Re-Analysis Validation Reports - Part 1, *ECMWF Re-Anal. Proj. Rep. Ser., Rep. 6*, Eur. Cent. for Medium-Range Weather Forecasts, Reading, England, 1997.

Thompson, L. G., Ice core evidence from Peru and China, in *Climate Since A. D. 1500*, edited by R. S. Bradley, and P. D. Jones, pp. 517-548, Routledge, New York, 1992.

von Storch, H., and F. W. Zwiers (Eds.), *Statistical Analysis in Climate Research*, Cambridge Univ. Press, New York, 1999.

von Storch, H., E. Zorita, and U. Cubasch, Downscaling of global climate change estimates to regional scales: An application to Iberian rainfall in wintertime, *J. Clim., 6*, 1161-1171, 1993.

Wigley, T. M. L., P. D. Jones, K. R. Briffa, and G. Smith, Obtaining sub-grid-scale information from coarse-resolution general circulation model output, *J. Geophys. Res., 95*, 1943-1953, 1990.

O. Åkesson, Swedish Meteorological and Hydrological Institute, 60176 Norrköping, Sweden.

L. Bengtsson and B. K. Reichert, Max-Planck-Institut für Meteorologie, Bundesstrasse 55, 20146 Hamburg, Germany. (e-mail: bengtsson@dkrz.de; reichert@dkrz.de)

(Received September 4, 1998; revised February 25, 1999; accepted April 14, 1999.)